RSC Advances

ROYAL SOCIETY OF CHEMISTRY

www.rsc.org/advances

Journal Name

RSCPublishing

ARTICLE

Al_2O_3-Gd_2O_3 double-films grown on graphene directly by H_2O-assisted atomic layer deposition

Cite this: DOI: 10.1039/x0xx00000x

Received 00th January 2012,
Accepted 00th January 2012

DOI: 10.1039/x0xx00000x

www.rsc.org/

Li Zheng,[ab] Xinhong Cheng*[a], Duo Cao, [ab] Dongliang Zhang,[ab] Zhongjian Wang, [a] Dawei Xu,[a] Chao Xia, [ab] Lingyan Shen[ab] and Yuehui Yu[a]

We demonstrate the direct Al_2O_3-Gd_2O_3 double-films growth onto graphene by H_2O-assisted atomic layer deposition (ALD) using a hexamethyl disilazane precursor {Gd[N(SiMe$_3$)$_2$]$_3$}. No defects are brought into graphene manifested by Raman spectra; the surface root-mean-square (RMS) roughness of Al_2O_3-Gd_2O_3 double-films is down to 0.8 nm, comparable with the morphology of pristine graphene; the films are compact and continuous, and the relative permittivity is around 11, which indicate H_2O-assisted ALD can prepare high quality of dielectric films on graphene.

Introduction

The outstanding electronic transport properties of graphene, including extremely high carrier mobilities (200,000 $cm^2V^{-1}s^{-1}$)[1-4], have generated significant interest in graphene-based nanoelectronics. In order to achieve graphene-based field-effect transistors (GFETs), the growth of high dielectric constant (high-κ) materials to act as the gate insulator is required.[5-7] Over the last decades, rare earth (RE) oxide based materials have been extensively studied because of their wide range of applications in optical devices, microelectronics, and magnetic devices.[8-10] The application of RE oxides as high-κ dielectrics in complementary metal oxide semiconductor (CMOS) devices has been investigated in detail, and Gd_2O_3 has shown great potential in this respect, exhibiting high dielectric constants (12-17), high thermal stabilities, and large band gaps (6.0 eV).[11-13] For applications in microelectronics, Gd_2O_3 films should be ultrathin, conformal, and pinhole-free with minimal disorder or traps. Atomic layer deposition (ALD) is the method of choice, as it allows excellent layer thickness control, low-temperature growth and uniform step coverage on complex device geometries. Nevertheless, due to the chemical inertness of graphene, the direct ALD growth of dielectric layers on bare graphene is rather challenging.

Several surface functionalization have been pursued by researchers to improve the uniformity of gate dielectric grown on graphene by ALD, including the deposition and oxidation of metal films, functionalization of graphene via ozone or nitrogen dioxide, and the spin-coating of polymer films as seeding layers.[14-18] However, these methods either introduce undesired impurities or break the chemical bonds in the graphene lattice, which results in significant degradation in carrier mobility.

In our previous work, we tried to deposit Al_2O_3 onto graphene directly by ALD.[19] The Al_2O_3films were compact and continuously covered graphene surface with a relative permittivity of 7.2 and a breakdown critical electrical field of 9 MV/cm. However, the permittivity of Al_2O_3 (7-9) is low, compared with RE oxide such as Gd_2O_3. Up till now, no related study on the investigation of direct Gd_2O_3 deposition onto graphene has been reported. This is an urgent issue to be addressed since it facilitates the achievement of graphene-based nano-electronic devices.

In this paper, we report on the direct H_2O-assisted ALD growth of both Gd_2O_3 films and Al_2O_3-Gd_2O_3 double-films on graphene surface without any functionalization. Raman spectra were performed to indicate both the thickness and quality of graphene before and after Gd_2O_3 films and Al_2O_3-Gd_2O_3 double-films deposition. Atomic force microscope (AFM) and high resolution transmission electron microscopy (HRTEM) were implemented to investigate the surface morphology and microstructure of Al_2O_3-Gd_2O_3 double-films on graphene, respectively. X-ray photoelectron spectroscopy (XPS) was applied to confirm all of elements present in the films. Spectroscopic ellipsometer and Capacitance–voltage (C-V) measurements were also carried out to show the optical and electrical quality of Al_2O_3-Gd_2O_3 double-films on graphene, respectively.

Experimental section

Graphene films were grown on Cu foil (0.025 mm, 99.8%) in a low pressure CVD system. During the graphene growth process, the quartz tube was maintained at 1050℃ for 60 min under the flow of 50 sccm H_2 and 10 sccm CH_4. After the growth, graphene samples were transferred onto Si substrates covered by 300 nm thickness of SiO_2. Acetone was used to remove PMMA and graphene was annealed at 200℃ for 3 hours under the flow of 10 sccm Ar and 50 sccm H_2 to remove the photoresist residue before ALD processes. The H_2 shielding could admirably prevent graphene from being oxidized by O_2 existing at the interface between graphene and substrates. The graphene flakes were monolayers characterized by Raman spectra and all the graphene samples were grown and transferred at the same condition.

The Gd_2O_3 films were deposited from $Gd[N(SiMe_3)_2]_3$ (purchased from J&K) and H_2O in a commercial ALD reactor (BENEQ TFS 200-124) maintained at a low level of base pressure by a vacuum pump (Adixen). $Gd[N(SiMe_3)_2]_3$ was preheated to 177℃ while H_2O was kept at room temperature. Four cycles of H_2O were introduced into ALD chamber before Gd_2O_3 films growth and acted as deposition sites on graphene. Details of the optimal H_2O dosage choice were discussed in our previous work.[19] Nitrogen gas (99.999% in purity) was used as a carrier gas at a flow rate of 200 sccm. The deposition process involved a pulse of $Gd[N(SiMe_3)_2]_3$ for 1s followed by a 10s purge. Subsequently, a pulse of H_2O for 1s followed by a 10s purge was applied. This process was repeated 100 times at 200℃. In this reaction, Gd_2O_3 formed and $NH(SiMe)_2$ was purged away (see eqn(1)).

$$2Gd[N(SiMe)_2]_3 + 3H_2O \rightarrow Gd_2O_3 + 6NH(SiMe)_2 \quad (1)$$

The thickness of Gd_2O_3 films was 20 nm confirmed by spectroscopic ellipsometer. For comparison, another sample of Gd_2O_3 films on graphene with an Al_2O_3 seed-like layer (Al_2O_3-Gd_2O_3 double-films) was also fabricated. Likewise, 4 cycles of pre-H_2O treatment were performed before Al_2O_3 growth and the Al_2O_3 seed-like layer (5 nm) was grown from $Al(CH_3)_3$ (TMA) and H_2O on graphene at 100℃ directly by ALD (see eqn(2)); subsequently, the chamber temperature was elevated to 200℃ and 11 nm of Gd_2O_3 films were deposited.

$$2Al(CH_3)_3 + 3H_2O \rightarrow Al_2O_3 + 6CH_4 \quad (2)$$

After growth of Gd_2O_3 films and Al_2O_3-Gd_2O_3 double-films, the samples were characterized by Raman spectra. In addition, AFM, TEM, XPS, spectroscopic ellipsometry and C-V measurements were also applied to estimate the dielectric films.

Results and discussion

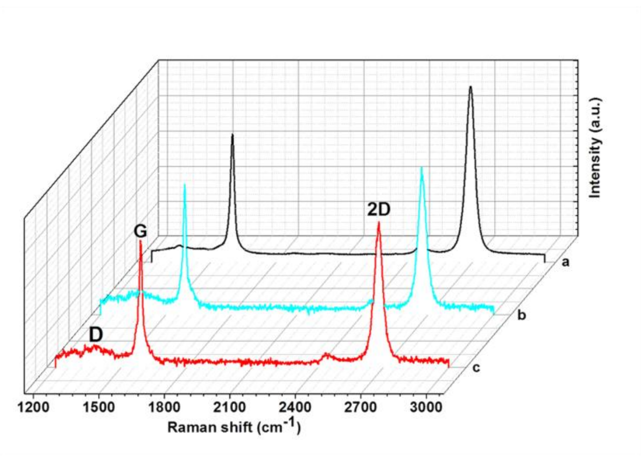

Fig. 1 Raman spectra of graphene with and without dielectric films. (a) Pristine graphene. (b) Graphene with 20 nm Gd_2O_3 deposited at 200℃. (c) Graphene with 5 nm Al_2O_3 deposited at 100℃ and 11 nm Gd_2O_3 deposited at 200℃.

Raman spectra were firstly utilized to determine both the quality and thickness of the graphene films with and without high-κ dielectrics growth. As shown in Fig. 1a, the pristine graphene had a weak D band peak at 1350 cm^{-1}, a G band peak at 1562 cm^{-1}, a sharp 2D band peak at 2675 cm^{-1} with a full width at half maximum (FWHM) of 50 cm^{-1} and an I_{2D}/I_G ratio greater than 1.3, indicating the graphene sample was monolayer with few defects. The weak D band peak was due to a little wrinkle generated during the transferring process. After high-κ dielectrics deposition, no raise of defect-related D-band was detected for both Gd_2O_3 (Figure 1b) and Al_2O_3-Gd_2O_3 (Figure 1c) samples, implying no defects or disorder were introduced into graphene by ALD processes. Raman spectra also revealed the phenomenon of G band blueshift and G peak upshift. The blueshift of G band was due to the compressive strain in graphene developed during the ALD process[20,21] and the upshift of G peak was due to the non-adiabatic removal of the Kohn anomaly from the Γ point.[22-24]

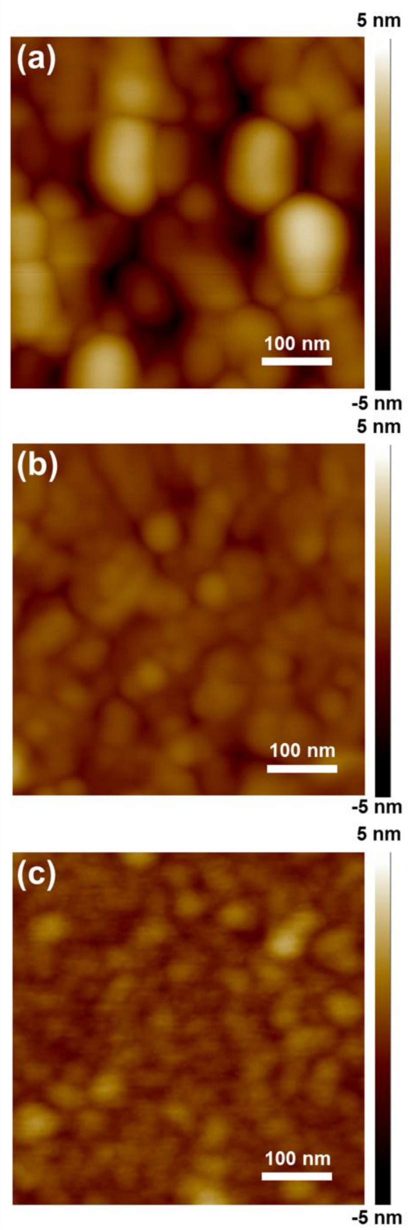

Fig. 2 AFM images (500×500nm^2) of graphene with and without high-κ films. (a) 20 nm Gd_2O_3 deposited at 200℃ on graphene. (b) 5 nm Al_2O_3 deposited at 100℃ and 11 nm deposited Gd_2O_3 at 200℃ on graphene. (c) Pristine graphene.

To determine whether an Al_2O_3 seed-like layer grown directly by ALD was beneficial for the quality of Gd_2O_3 films on graphene, samples were measured by AFM. As shown in Figure 2a, the surface RMS roughness of Gd_2O_3 films directly deposited on graphene was 2.7 nm. Although Gd_2O_3 films could be grown directly on graphene with assistant of physically absorbed H_2O molecules, pin-holes were detective and the surface morphology was rough. In order to grow Gd_2O_3 films from $Gd[N(SiMe_3)_2]_3$ by ALD, the chamber temperature should be over 177℃ due to the high sublimation temperature of $Gd[N(SiMe_3)_2]_3$. However, the surface of graphene had no dangling bonds and high temperature prevented uniform distribution of physically absorbed H_2O molecules on graphene, which resulted in insufficient deposition sites for Gd_2O_3 and led to pinholes in Gd_2O_3 films. When an Al_2O_3 seed-like layer was deposited directly on graphene by ALD at 100 ℃, the subsequent Gd_2O_3 films grown at 200℃ were continuous and pinhole-free. As shown in Figure 2b, the surface RMS roughness of Al_2O_3-Gd_2O_3 double-films on graphene was down to 0.8 nm, which was comparable with the morphology of pristine graphene with a RMS roughness of 0.6 nm (Figure 2c). As our previous work reported,[19] 100℃ was suitable for direct ALD Al_2O_3 growth on graphene with 4 cycles of pre-H_2O treatment. In addition, $Al(CH_3)_3$ was more active than $Gd[N(SiMe_3)_2]_3$ and Al_2O_3 molecules were smaller than Gd_2O_3 molecules; it was more easy to directly deposit continuous Al_2O_3 than Gd_2O_3 onto graphene. Therefore, for Gd_2O_3 films directly deposited on graphene by ALD, an Al_2O_3 seed-like layer was feasible and it could enhance the property of Gd_2O_3 films.

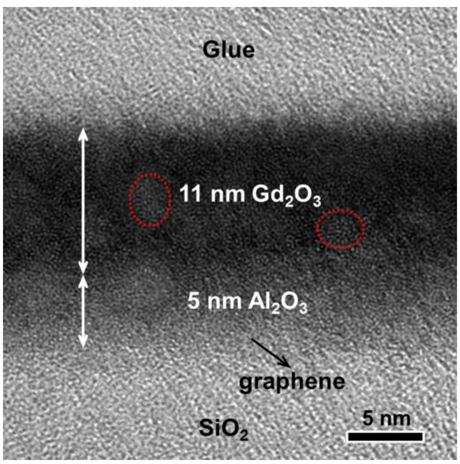

Fig. 3 A HRTEM image of Al_2O_3-Gd_2O_3 double-films on graphene. Al_2O_3 deposited at 100℃ was 5 nm and Gd_2O_3 deposited at 200℃ was 11 nm.

Moreover, in order to further indiate the beneficial effect of an Al_2O_3 seed-like layer, HRTEM was performed to character the cross-sectional structure of Al_2O_3-Gd_2O_3 double-films on graphene deposited directly by H_2O-assisted ALD. As shown in Figure 3, the thicknesses of Al_2O_3 and Gd_2O_3 films were 5 nm and 11 nm, respectively. The Al_2O_3 films were amorphous while parts of the Gd_2O_3 films were polycrystalline (red dotted circles in Figure 3). The easy crystalline nature of Gd_2O_3 was due to its low crystallization temperature. It was particularly worth mentioning that in spite of the loose Al_2O_3 films, the Gd_2O_3 films were compact. During the ALD process, Al_2O_3 could act as a seed-like layer, which was beneficial to the compactness of the subsequent Gd_2O_3 films. In our previous study, for purpose of investigating whether the thickness of an Al_2O_3 seed-like layer could be reduced, we prepared five controlled samples with an Al_2O_3 seed-like layer of 1 nm, 2 nm, 3 nm, 4 nm and 5 nm, respectively. Through contrast experiments, we found that the Al_2O_3 seed-like layer could be reduced to 4 nm. Details of the discussion about how thin the Al_2O_3 seed-like layer can go could be found in our previous work.[19]

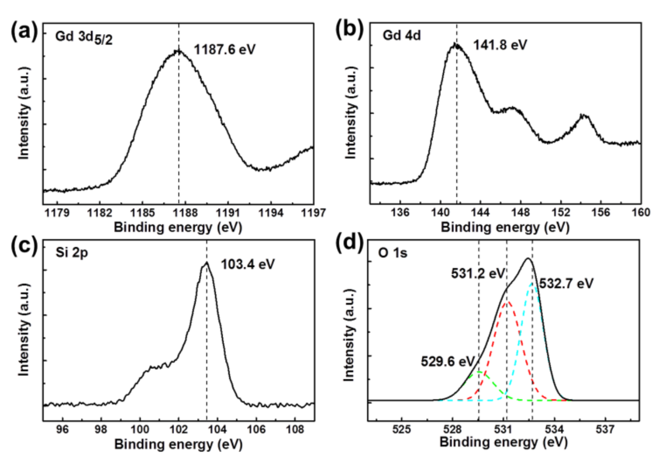

Fig. 4 XPS analysis of Al_2O_3-Gd_2O_3 double-films on graphene: Gd $3d_{5/2}$ (a), Gd 4d (b), Si 2p (c) and O 1s (d).

Fig. 4 demonstrates the results of XPS analysis to confirm all of elements present in the films. The binding energy was calibrated by centering the C 1s peak at 284.5 eV. The Gd $3d_{5/2}$ peak located at 1187.6 eV (Fig. 4a), separated by 1045.8 eV from the Gd 4d peak located at 141.8 eV (Fig. 4b), indicating the existence of Gd^{3+}. In addition to Gd^{3+}, the Si 2p peak located at 103.4 eV was also detected. The existence of Si in Gd_2O_3 films was probably generated from the oxidizing of by-products in eqn 1 during the ALD process.

$$NH(SiMe)_2 + 2H_2O \rightarrow SiO_2 + NH_5Me_2 \quad (3)$$

As shown in eqn 3, the by-product, $NH(SiMe)_2$, in eqn (1) could react with H_2O, leading to the formation of SiO_2 and this result could also be concluded from the analysis of O 1s peak illustrated in Fig. 4d. The O 1s peak was asymmetric and further deconvolution revealed three distinct components. The two stronger peak locating at 531.2 eV and 532.7 eV originated from Gd−O and Si-O bonds, respectively, and the weak peak at 529.6 eV associated with OH^- hydroxyl groups due to the incomplete reaction of $Gd[N(SiMe_3)_2]_3/H_2O$. The atomic radio of Si/Gd is about 0.96, indicating high concentration doping of Si in Gd_2O_3 film.

Spectroscopic ellipsometry was applied for the investigation of the optical constants (refractive index n, absorption coefficient α, and complex permittivity ε) of Al_2O_3-Gd_2O_3 double-films on graphene. The refractive index n and extinction coefficient k of Al_2O_3-Gd_2O_3 double-films were directly obtained from ellipsometry measurements. As shown in Fig. 5a, the refractive index n of Al_2O_3-Gd_2O_3 double-films on graphene presented increasing tendency with increase of wavelengths λ and it was approximately 3.2 in the visible region. The absorption coefficients α was calculated from the extinction coefficients k by the following formula:

$\alpha = 4\pi k / \lambda$. As illustrated in Fig. 5b, the absorption coefficients α of Al_2O_3-Gd_2O_3 double-films demonstrated increasing tendency with increase of the photon energy from 1.0 eV to 3.0 eV (1100 nm-400 nm) and had an absorption peak in the range of 3.0 eV to 5.0 eV (400 nm-250 nm). The complex permittivity ε ($\varepsilon = \varepsilon_r - i\varepsilon_i$) of Al_2O_3-Gd_2O_3 double-films on graphene could also be calculated from refractive index n and extinction coefficients k according to the following formulas: $\varepsilon_r = n^2 - k^2$ and $\varepsilon_i = 2nk$, where ε_r and ε_i are the real part and imaginary part of the complex permittivity, respectively (Fig. 5c). It was interesting to note that the real part of the complex permittivity ε_r was negative in the near ultraviolet region (from 220 nm to 400 nm), indicating that graphene/Al_2O_3-Gd_2O_3 might act as a meta material and applied to novel optical devices. The negative value of ε_r was due to the sudden enhancement of the extinction coefficients k in the near ultraviolet region as shown in the inset of Fig. 5c, and this enhancement was determined by the intrinsic properties of graphene/Al_2O_3-Gd_2O_3.

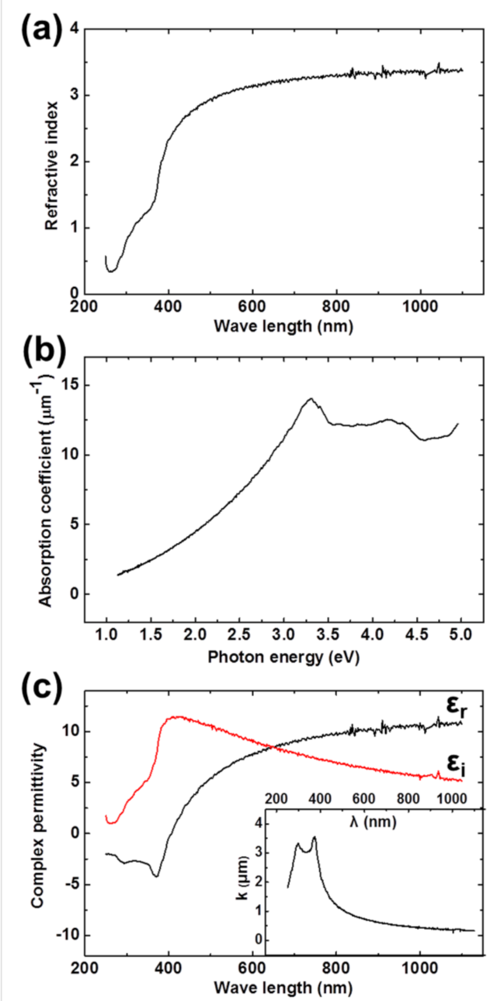

Fig. 5 Optical properties analysis of Al_2O_3-Gd_2O_3 double-films on graphene by spectroscopic ellipsometry: refractive index (a), absorption coefficient (b) and complex permittivity (c).

C-V measurements were also employed to estimate the electrical properties of Al_2O_3-Gd_2O_3 double-films on graphene. A metal-oxide-graphene (MOG) structure was adopted in the electrical analysis shown in Figure 6a. The areas of each electrode were 0.01 mm^2 and the distance between two electrodes was 0.8 mm. The actual capacitance value was double of the measured one due to the series connection of two same capacitors. Fig.6b showed the accurate model of MOG structure (left) and the series circuit model [25] (middle) employed in the C-V measurements. The impedance of a MOG capacitor was given by

$$Z = R_s + \frac{R_c(1 - j2\pi fCR_c)}{1 + (2\pi fCR_c)^2} \qquad (4)$$

where R_c included the ac conductance induced resistances arising from interface traps, and R_s included all of the series resistances. The impedance could also be obtained from the following formula when a series circuit model was performed:

$$Z = R_m + \frac{1}{j2\pi fC_m} \qquad (5)$$

where R_m and C_m referred to measured values. Equating the imaginary parts of equations (4) and (5), one could obtain

$$\frac{1}{2\pi fC_m} = \frac{2\pi fCR_c^2}{1 + (2\pi fCR_c)^2} \qquad (6)$$

A dual-frequency method[26] was introduced to correct for series resistance effects and to determine accurately the capacitance of Al_2O_3-Gd_2O_3 films. Measuring the capacitance at two different frequencies, substituting into (6) for each frequency, subtracting, and solving for C, one could obtain

$$C = \frac{f_1^2 C_1 - f_2^2 C_2}{f_1^2 - f_2^2} \qquad (7)$$

where C_1 (C_2) referred to the values measured at the frequency f_1 (f_2).

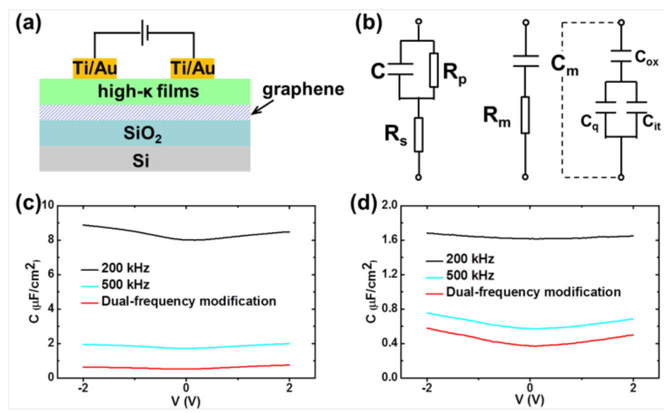

Fig. 6 (a) The MOG structure. (b) The accurate model (left) and the series model (right) of MOG structure. (c), (d) C-V measurements of Gd_2O_3 films and Al_2O_3- Gd_2O_3 double-films performed at different frequencies: 200 kHz (curve a), 500 kHz (curve b), and modified by dual-frequency method (curve c), respectively.

The measured capacitance (C_m) was consisted of three components: the oxide capacitance (C_{ox}), the quantum capacitance of graphene (C_q) and the capacitance induced by interface states (C_{it}), as shown in Fig.6b (right). C-V measurements of Gd_2O_3 films and Al_2O_3-Gd_2O_3 double-films were both implemented at two frequencies (200 kHz and 500 kHz) and modified by equation (7) as shown in Fig. 6c and 6d, respectively. All the C-V measurements showed the expected broad V-shape induced by the quantum capacitance (C_q) of graphene,[27,28] indicating C_{it} did not play a major role in the measured capacitance (C_m), or the V-shape curve would not be detected. In addition, C_q was in parallel to C_{it}, while both of them were in series to the oxide capacitance (C_{ox}), and C_{ox} was approximately an order of magnitude lower than C_q at the bias away from the Dirac Point of graphene. Thus, the measured capacitance at $\pm$ 2V was close to C_{ox}. The capacitances of Gd_2O_3 films and Al_2O_3-Gd_2O_3 double-films were 0.64 $\mu F/cm^2$ and 0.58 $\mu F/cm^2$, while the relative permittivities were 15 and 11, respectively. The permittivity reduction of Al_2O_3-Gd_2O_3 double-films was due to the relatively small permittivity of Al_2O_3 (7-9). However, the introduction of an Al_2O_3 seed-like layer was beneficial to both the surface morphology and compactness of subsequently deposited Gd_2O_3 films.

Conclusions

In summary, we have directly deposited Gd_2O_3 films and Al_2O_3-Gd_2O_3 double-films onto pristine graphene by ALD. No additional defects are introduced into graphene after high-κ films deposition. The introduction of an Al_2O_3 seed-like layer benefits both the surface morphology and compactness of subsequently deposited Gd_2O_3 films. The surface RMS of Al_2O_3-Gd_2O_3 double-films is down to 0.8 nm and the relative permittivity is around 11, which indicate high quality of high-κ films. This technique provides scientific guidance in fabricating novel graphene-based electronic devices.

Acknowledgements

This work is funded by the National Natural Science Foundation of China (Grant No. 11175229).We would like to thank Pro. Zengfeng Di, Dr. Gang Wang, Dr. Xiaohu Zheng and Dr. Haoran Zhang for their generous help.

Notes and references

[a]*State Key Laboratory of Functional Materials for Informatics, Institute of Microsystem and Information Technology, Chinese Academy of Sciences, Shanghai 200050, China. E-mail: xh_cheng@mail.sim.ac.cn*
[b]*University of Chinese Academy of Sciences, Beijing 100049, China.*

1 K. S. Novoselov, A. K. Geim, S. V. Morozov, D. Jiang, Y. Zhang, S. V. Dobonos, I. V. Grigorieval, and A. A. Firsov, *Science*, 2004, **306**, 666-669.
2 A. A. Balandin, S. Ghosh, W. Bao, I. Calizo, D. Teweldebrhan, F. Miao, and C. N. Lau, *Nano Lett.*, 2008, **8**, 902-907.
3 M. D. Stoller, S. Park, Y. Zhu, J. An, and R. S. Ruoff, *Nano Lett.*, 2008, **8**, 3498-3502.
4 C. Lee, X. Wei, J. W. Kysar, and J. Hone, *Science*, 2008, **321**, 385-388.
5 B. H. Lee, J. Oh, H. H. Tseng, R. Jammy, and H. Huff, *Mater. Today*, 2006, **9**, 32-37.
6 L. Wang, J. J. Travis, A. S. Cavanagh, X. Liu, S. P. Koenig, P. Y. Huang, S. M. George, and J. S. Bunch, *Nano Lett.*, 2012, **12**, 3706-3710.
7 W. C. Shin, T. Y. Kim, O. Sul, and B. J. Cho, *Appl. Phys. Lett.*, 2012, **101**, 033507.
8 J. C. G. Buenzil, and C. Piguet, *Chem. Soc. Rev.*, 2005, **34**, 1048-1077.
9 J. Kido, and Y. Okamoto, *Chem. Rev.*, 2002, **102**, 2357-2368.
10 J. Robertson, Eur. Phys. *J. Appl. Phys.*, 2004, **28**, 2357.
11 W. H. Chang, C. H. Lee, Y. C. Chang, P. Chang, M. L. Huang, Y. J. Lee, C. Hsu, J. M. Hong, C. C. Tsai, J. R. Kwo, and M. Hong, *Adv. Mater.*, 2009, **21**, 4970-4974.
12 A. P. Milanov, K. Xu, A. Laha, E. Bugiel, R. Ranjith, D. Schwendt, H. J. Osten, H. Parala, R. A. Fischer, and A. Devi, *J. Am. Chem. Soc.*, 2010, **132**, 36-37.
13 K. Xu, R. Ranjith, A. Laha, H. Parala, A. P. Milanov, R. A. Fischer, E. Bugiel, J. Feydt, S. Irsen, T. Toader, C. Bock, D. Rogalla, H. Osten, U. Kunze, and A. Devi, *Chem. Mater.*, 2012, **24**, 651-658.
14 M. J. Hollander, M. LaBella, Z. R. Hughes, M. Zhu, K. A. Trumbull, R. Cavalero, D. W. Snyder, X. J. Wang, E. Hwang, S. Datta, and J. A. Robinson, *Nano Lett.*, 2011, **11**, 3601-3607.
15 B. Lee, G. Mordi, M. J. Kim, Y. J. Chabal, E. M. Vogel, R. M. Wallace, K. J. Cho, L. Colombo, and J. Kim, *Appl. Phys. Lett.*, 2010, **97**, 043107.
16 Y. Xuan, Y. Q. Wu, T. Shen, M. Qi, M. A. Capano, J. A. Cooper, and P. D. Ye, *Appl. Phys. Lett.*, 2008, **92**, 013101.
17 D. B. Farmer, H. Y. Chiu, Y. M. Lin, K. A. Jenkins, F. N. Xia, and P. Avouris, *Nano Lett.*, 2009, **9**, 4474-4478.
18 Y. M. Lin, K. A. Jenkins, A. V. Garcia, J. P. Small, D. B. Farmer, and P. Avouris, *Nano Lett.*, 2009, **9**, 422-426.
19 L. Zheng, X. Cheng, D. Cao, G. Wang, Z. Wang, D. Xu, C. Xia, L. Shen, Y. Yu,and Da. Shen, *ACS Appl. Mater. Interfaces*, 2014, **6**, 7014-7019.
20 T. M. G. Mohiuddin, A. Lombardo, R. R. Nair, A. Bonetti, G. Savini, R. Jalil, N. Bonini, D. M. Basko, C. Galiotis, N. Marzari, K. S. Novoselov, A. K. Geim, and A. C. Ferrari, *Phys. Rev. B*, 2009, **79**, 205433.
21 J. A. Robinson, M. LaBella, K. A. Trumbull, X. Weng, R. Cavelero, T. Daniels, Z. Hughes, M. Hollander, M. Fanton, and D. Snyder, *ACS Nano*, 2010, **4**, 2667-2672.
22 S. Pisana, M. Lazzeri, C. Casiraghi1, K. S. Novoselov, A. K. Geim, A. C. Ferrari1, and M. Maur, *Nat. Mater.*, 2007, **6**, 198-201.
23 A. Das, S. Pisana, B. Chakraborty, S. Piscanec, S. K. Saha1, U. V. Waghmare, K. S. Novoselov, H. R. Krishnamurthy, A. K. Geim, A. C. Ferrari, and A. K. Sood, *Nat. Nanotechnol.*, 2008, **3**, 210-215.
24 H. Xu, Y. B. Chen, J. Zhang, and H. L. Zhang, *Small*, 2012, **8**, 2833-2840.
25 K. J. Yang and C. Hu, *IEEE Trans. Electron Devices*, 1999, **46**, 1500-1501.
26 Z. Luo and T. P. Ma, *IEEE Electr. Device L.*, 2004, **25**, 655-657.
27 T. Fang, A. Konar, H. Xing, and D. Jena, *Appl. Phys. Lett.*, 2007, **91**, 092109.
28 J. Xia, F. Chen, J. Li, and N. Tao, *Nat. Nanotechnol.*, 2009, **4**, 505-509.

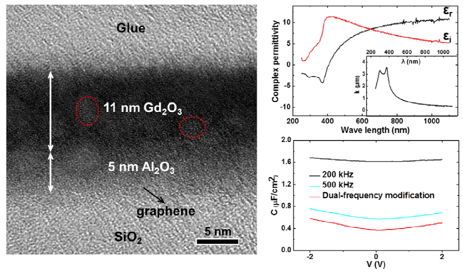

Al_2O_3-Gd_2O_3 double-films were directly grown on graphene with assistance of H_2O by atomic layer deposition without any functionalization.